

Optical phonons in the orthorhombic double-chain $\text{Sr}_{1-x}\text{Ca}_x\text{CuO}_2$ ($x=0, 0.5$)

M. V. Abrashev,* A. P. Litvinchuk, and C. Thomsen

Institut für Festkörperphysik, Technische Universität Berlin, Hardenbergstrasse 36, 10623 Berlin, Germany

V. N. Popov*

Laboratoire de Physique des Solides, Université Pierre et Marie Curie, 4 Place Jussieu, 75252 Paris, France

(Received 13 August 1996)

We report micro-Raman and far-infrared reflectivity spectra obtained from the two members SrCuO_2 and $\text{Sr}_{0.5}\text{Ca}_{0.5}\text{CuO}_2$ of the solid solution $\text{Sr}_{1-x}\text{Ca}_x\text{CuO}_2$ with orthorhombic chain structure. The analysis of the spectra is based on the similarity between the investigated structure and related copper oxides, which contain the same type of copper-oxygen chains. The assignment of the observed lines to atomic vibrations is supported by shell model lattice-dynamics calculations. [S0163-1829(97)05610-5]

I. INTRODUCTION

The interest in the strontium cuprates has increased considerably after the synthesis of tetragonal SrCuO_2 under high pressure. This compound has the simplest structure (infinite two-dimensional CuO_2 layers) among all high-temperature superconductors and a critical temperature up to 100 K.¹ Recently, using the same high-pressure techniques, new homologous series $\text{Sr}_{n+1}\text{Cu}_n\text{O}_{2n+1+\delta}$ and $\text{Sr}_n\text{Cu}_{n+1}\text{O}_{2n+1}$ were obtained.² At ambient pressure only three strontium cuprates have been synthesized: Sr_2CuO_3 , SrCuO_2 , and $\text{Sr}_{14}\text{Cu}_{24}\text{O}_{41}$.^{3,4} They are all orthorhombic and contain single CuO_3 chains, double Cu_2O_4 chains, and corner-sharing Cu_2O_3 double chains, respectively. The former two phases are insulators and one-dimensional spin-1/2 antiferromagnets,^{5,6} but the latter is a p -type self-doped material. Kato *et al.*⁷ have shown that when varying the content of the alkaline earth elements in $\text{Sr}_{14-x}\text{A}_x\text{Cu}_{24}\text{O}_{41}$ ($A = \text{Ba}, \text{Ca}$) it is possible to redistribute holes between the two types of chains in the structure and to achieve values close to the ones necessary for superconductivity. It was theoretically predicted that corner-sharing double copper-oxygen chains through hole doping may exhibit high- T_c superconductivity.⁸ On the other hand, these compounds are interesting from a purely technological point of view, because of their existence in the Bi-Sr-Ca-Cu-O ceramics.

In this paper we investigate vibrational properties of $\text{Sr}_{1-x}\text{Ca}_x\text{CuO}_2$ ($x=0, 0.5$) using micro-Raman and far-infrared (FIR) spectroscopies. The structure of the parent compound SrCuO_2 is orthorhombic, space group $Cmcm$ (D_{2h}^{17} no. 63), $Z=4$,⁹ and it has recently been refined by Matsushita *et al.*¹⁰ It contains double Cu_2O_4 chains separated by double rock-salt-type Sr-O layers (see Fig. 1). The determined maximal solubility x_{max} of Ca in $\text{Sr}_{1-x}\text{Ca}_x\text{CuO}_2$ was shown to be in the range $0.50 \leq x_{\text{max}} \leq 0.75$.^{3,4,11}

The analysis of the vibrational spectra was performed using the similarity between the investigated structure and two structures with well-known spectra. These are $\text{Ca}_{2-x}\text{Sr}_x\text{CuO}_3$ (with the same type Sr/Ca-O rock-salt layer, but with single CuO_3 chains) (Refs. 12–14) and

$\text{YBa}_2\text{Cu}_4\text{O}_8$ (with the same double Cu_2O_4 chains).¹⁵ The assignment of the observed lines in the spectra to definite atomic vibrations is supported by lattice-dynamics calculations based on a shell model.

II. EXPERIMENT

The $\text{Sr}_{1-x}\text{Ca}_x\text{CuO}_2$ ($x=0, 0.5$) samples were prepared using a standard solid state reaction technique. Appropriate amounts of SrCO_3 , CaCO_3 , and CuO for the nominal ratios were mixed and heated in air at 850 °C for 24 h, grinded, and again heated at 900 °C for 24 h. The as-obtained materials were pressed into 1 g pellets and sintered at 900 °C for

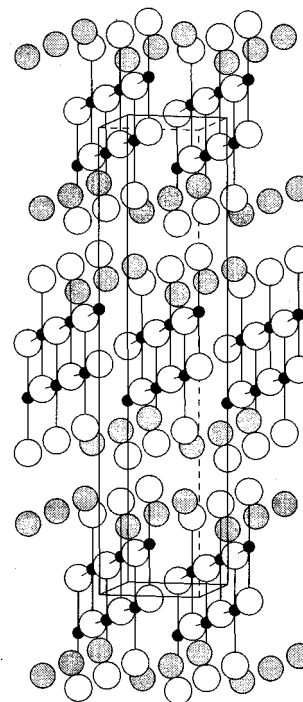


FIG. 1. The crystal structure and an unit cell of $\text{Sr}_{1-x}\text{Ca}_x\text{CuO}_2$. The large gray circles are Sr/Ca atoms, the large white circles are oxygen atoms, the small black circles are Cu atoms. The b axis is vertical, the c axis is parallel to the copper-oxygen chains.

24 h and then furnace cooled to room temperature. For the microscopic measurements the pellets were polished using 5 μ and 1 μ diamond pastes and then ultrasonically cleaned in an ethanol bath. We note that the samples are not as hygroscopic as their $\text{Sr}_{2-x}\text{Ca}_x\text{CuO}_3$ analogs.

The lattice parameters were determined from x-ray powder diffractograms, obtained with a URD-6 powder diffractometer (Cu K_α radiation). They are $a = 3.5801$ Å, $b = 16.352$ Å, $c = 3.916$ Å for SrCuO_2 and $a = 3.4546$ Å, $b = 16.146$ Å, $c = 3.8786$ Å for $\text{Sr}_{0.5}\text{Ca}_{0.5}\text{CuO}_2$. These values are close to those reported elsewhere.^{3,10,11} The samples studied are monophasic.

The Raman spectra were measured using a Labram spectrometer equipped with an optical microscope. An 100 \times objective was used to both focus the incident laser beam into a spot of 1–2 μm diameter and collect the scattered light in backward scattering geometry. A 632.8 nm He-Ne laser line was used for excitation. The procedure to identify the crystal directions in the measured microcrystal surfaces is discussed below.

The near-normal incidence far-infrared spectra were measured with a Bruker-66V Fourier-transform interferometer in the range 50–8000 cm^{-1} . A gold mirror was used as a reference. All measurements were performed at room temperature.

III. RESULTS AND DISCUSSION

A. Classification of the Γ -point phonons

Crystallographic data on $\text{Sr}_{1-x}\text{Ca}_x\text{CuO}_2$ show that all atoms [Sr/Ca , Cu , O_{Cu} (the oxygen atoms within the Cu-O chains) and O_{Sr} (the oxygen atoms from the Sr-O layers)] occupy one and the same type of positions of the space group $Cmcm$, namely $4c$ (0, y , 1/4) with the site symmetry C_{2v}^y . This leads to the existence of 21 optical phonons: $4A_g$, $4B_{1g}$, $4B_{3g}$, $3B_{1u}$, $3B_{2u}$, and $3B_{3u}$. The first three types are Raman active only, the second three types are IR active only. The B_{3g} and B_{1u} modes are vibrations along the c axis, B_{1g} and B_{3u} modes along the a axis, A_g and B_{2u} modes along the b axis (note that the displacement directions of the Raman-active modes are different here from typical orthorhombic superconductors, e.g., $\text{YBa}_2\text{Cu}_3\text{O}_7$, due to the choice of the coordinate system). The Raman-active A_g modes are allowed only in parallel xx , yy and zz polarizations of the incident and scattered light, B_{1g} modes only in crossed xy polarization, and B_{3g} modes only in crossed yz polarization.

To separate the lines observed in the polarized Raman spectra by symmetry it is necessary to identify the crystal directions of the observed microcrystal surfaces. In the case of orthorhombic crystals this is not trivial. Moreover, due to the base centering of the lattice the typical form of the crystals is an eight-faced prism (see Fig. 1 in Ref. 10). To resolve this problem we used initially the fact that the intensity of the strongest A_g lines in polarizations along the three crystal axes are rather different (see Figs. 2 and 3). In addition we used two other facts: first, that due to the chain crystal structure, the microcrystals have a needle-like form (which identifies the c axis), and second that in one type crossed polarization (xz) there are no Raman-allowed modes (identifying

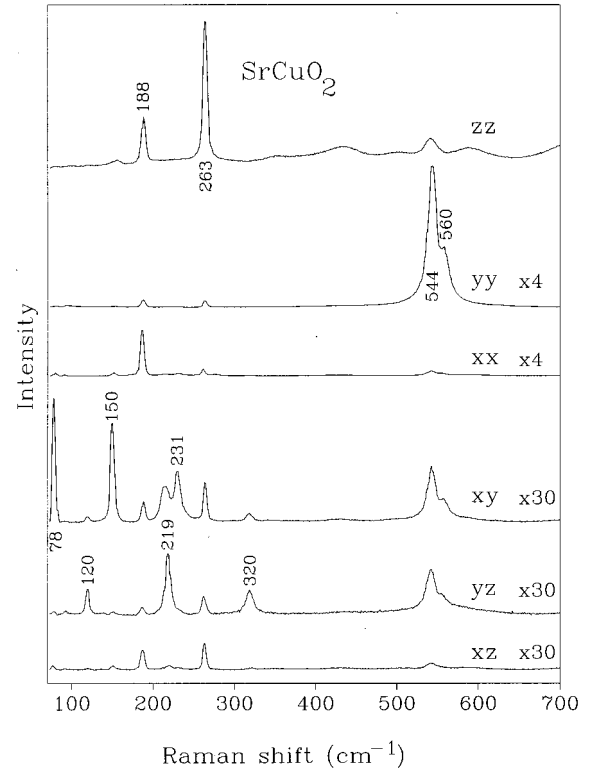


FIG. 2. Polarized Raman spectra obtained from three types of differently oriented surfaces of SrCuO_2 microcrystals. For better comparison some spectra are multiplied by a number, indicated in the figure. $\lambda_L = 632.8$ nm.

the b axis). The Raman spectra obtained in parallel polarization along the as-determined x , y , and z directions for SrCuO_2 are in very good agreement with those published recently in Ref. 14 for a single crystal.

B. Description of the model used for lattice-dynamics calculations

The model applied is a shell model with parameters derived as described in Ref. 16. This model is appropriate for the perovskite-like oxides because, in accordance with their predominant ionicity, the interionic interactions are represented as sums of long-range Coulomb potentials and short-range (SR) potentials. The latter are chosen here in the Born-Mayer-Buckingham form

$$V = a \exp(-br) - c/r^6. \quad (3.1)$$

Here a , b , and c are parameters, and r is the interionic separation. The ionic polarizability is also accounted for in the shell model using the simple picture of an ion as a point charged core coupled with a force constant k to a charged massless shell with charge Y around it. The free ionic polarizability α is given by

$$\alpha = Y^2/k. \quad (3.2)$$

Following the approach given in Ref. 16, we use the model parameters, which have been derived for other well-studied compounds and tabulated therein. The values of the model parameters are listed in Table I.

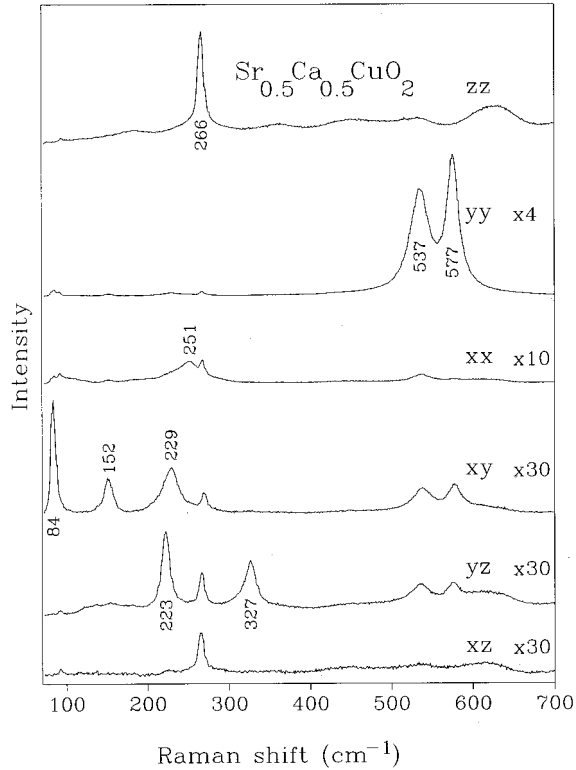


FIG. 3. Polarized Raman spectra obtained from three types of differently oriented surfaces of $\text{Sr}_{0.5}\text{Ca}_{0.5}\text{CuO}_2$ microcrystals. For better comparison some spectra are multiplied by a number, indicated in the figure. $\lambda_L = 632.8$ nm.

C. Raman-active phonons

Typical spectra obtained from differently oriented surfaces of SrCuO_2 and $\text{Sr}_{0.5}\text{Ca}_{0.5}\text{CuO}_2$ are presented in Figs. 2 and 3, respectively. A comparison between the experimental and calculated frequencies and their assignment is listed in Table II. First we discuss the four strong A_g lines. Their frequencies in the case of SrCuO_2 coincide with those published in Ref. 14. The lowest line at 188 cm^{-1} (in SrCuO_2) we assign to the Sr A_g mode. The same mode in $\text{Sr}_{0.5}\text{Ca}_{0.5}\text{CuO}_2$ is expected at a higher frequency due to the decreasing average mass and ionic radius of the ions in the Sr/Ca position. We conclude that the respective line is the one at 251 cm^{-1} . This large shift is in agreement with a similar shift of the corresponding A_g mode in $\text{Ca}_{2-x}\text{Sr}_x\text{CuO}_3$, which contains the same type rock-salt Sr/Ca-O layers. In Sr_2CuO_3 it is at 205 cm^{-1} ,¹⁴ whereas in Ca_2CuO_3 it was observed at 311 cm^{-1} .¹³ We note that in $\text{Sr}_{0.5}\text{Ca}_{0.5}\text{CuO}_2$ this line is strongly broadened. This is a consequence of the substitution in the corresponding sublattice.

TABLE II. Experimental and calculated frequencies (in cm^{-1}) and an assignment of the Raman-active modes.

Type	SrCuO_2		$\text{Sr}_{1-x}\text{Ca}_x\text{CuO}_2$		Assignment
	Expt.	Calc.	Expt.	Calc.	
A_g	188	178	251	213	Sr/Ca
A_g	263	263	266	255	Cu
A_g	544	530	537	527	O_{Sr}
A_g	560	547	577	548	O_{Cu}
B_{1g}	78	75	84	83	Librational
B_{1g}	150	151	152	160	Cu
B_{1g}	-	173	-	178	$\text{O}_{\text{Cu}}, \text{O}_{\text{Sr}}$ out of phase
B_{1g}	231	266	229	278	O_{Sr}
B_{3g}	120	116	-	138	Sr/Ca
B_{3g}	219	219	223	229	Cu
B_{3g}	320	352	327	361	O_{Sr}
B_{3g}	-	539	-	562	O_{Cu}

The strongest line in both compounds (263 cm^{-1} and 266 cm^{-1}) is the Cu A_g mode. Its analog in $\text{YBa}_2\text{Cu}_4\text{O}_8$, a compound containing similar double Cu-O chains, is at 248 cm^{-1} .¹⁵

It is rather difficult to identify the origin of the two high-frequency A_g lines because their frequencies are very close. In general, the same symmetry and a small frequency separation of two modes is a prerequisite for their resonant interaction. Based on the lattice-dynamics calculations, however, we assign the lower frequency mode to the O_{Sr} mode and the higher one to the O_{Cu} A_g vibration. An additional argument is that only the lower one exhibits a significant broadening in the spectra of $\text{Sr}_{0.5}\text{Ca}_{0.5}\text{CuO}_2$ (Fig. 3). The corresponding A_g mode of O_{Cu} in $\text{YBa}_2\text{Cu}_4\text{O}_8$ lies at 605 cm^{-1} .¹⁵ We note also that the A_g modes of Sr/Ca and O_{Sr} have the same polarization properties as their counterparts in $\text{Ca}_{2-x}\text{Sr}_x\text{CuO}_3$.¹²⁻¹⁴

The remaining broad peaks and strong background (both with A_g symmetry) up to 1300 cm^{-1} , observed only in parallel polarization along the chains (here zz), do not have a Raman-allowed one-phonon origin and will be discussed elsewhere. Similar complex features have been observed in single-chain $\text{Ca}_{2-x}\text{Sr}_x\text{CuO}_3$, too.¹²⁻¹⁴

The nondiagonal modes in all mixed copper oxides have been relatively little investigated compared to the diagonal ones because of their rather low intensity. In our case, however, we succeeded in clearly observing six out of eight allowed modes. Since some of them have analogs in the layered cuprates, where their assignment is rather tentative, we can use this similarity to revise the assignment of part of them in the latter compounds. The lattice-dynamics calculations show that the lines at 150 (152) cm^{-1} and 219 (223)

TABLE I. Parameters used in the shell model. The O-O SR potential is given from Ref. 17.

Ion	Z ($ e $)	Y ($ e $)	α (\AA^3)	Ionic pair	a (eV)	b (\AA^{-1})	c (eV \AA^6)
Sr	1.90	3.0	2.5	Sr-O	939	2.682	0
Sr/Ca	1.90	3.0	2.5	Sr/Ca-O	978	2.743	0
Cu	1.90	3.0	1.3	Cu-O	1150	3.550	0
O	-1.90	-3.0	2.0	O-O	22764	6.711	20.37

cm^{-1} in SrCuO_2 ($\text{Sr}_{0.5}\text{Ca}_{0.5}\text{CuO}_2$) should be assigned to the B_{1g} and B_{3g} Cu modes, respectively. This encourages us to draw conclusions about the typical vibrational frequencies of copper in a square CuO_4 and a pyramidal CuO_5 environment.

The vibration perpendicular to the base of the oxygen pyramid has A_{1g} (A_g) symmetry in tetragonal (orthorhombic) layered cuprates, and its frequency varies only slightly ($140\text{--}160\text{ cm}^{-1}$) for different materials. In our case this vibration has B_{1g} symmetry and similar frequency even without the fifth ‘‘apex’’ oxygen. This makes it plausible to call this vibration purely ‘‘bending.’’ The other ‘‘stretching’’ Cu vibrations within CuO_4 square possess, naturally, rather higher frequencies. Indeed, in our compounds the ‘‘stretching’’ Cu vibrations have frequencies 219 (223) cm^{-1} (for the B_{3g} mode) and 263 (266) cm^{-1} (for the A_g mode). The differences in frequencies of these modes correlate with the Cu-O distances along z (1.96 and 1.96 \AA) and y (1.93 and 1.91 \AA) directions. Other reported frequencies of the stretching vibration of square-coordinated copper are in the same region: 248 cm^{-1} in $\text{YBa}_2\text{Cu}_4\text{O}_8$,¹⁵ 251 cm^{-1} in $\text{PrBa}_2\text{Cu}_4\text{O}_8$,¹⁸ 248 cm^{-1} in $\text{H}_{1.0}R\text{Ba}_2\text{Cu}_3\text{O}_{7-\delta}$ ($R = \text{Y, Gd}$).¹⁹

On the other hand, the same type Cu-stretching vibrations in the CuO_5 pyramids have E_g symmetry (for tetragonal compounds) or B_{2g}/B_{3g} symmetry (for orthorhombic ones). McCarty *et al.*,²⁰ based on the lattice-dynamics calculations of Kress *et al.*,²¹ assigned these modes to two weak lines near 140 cm^{-1} . In a recent publication of Misochko *et al.*,²² however, this assignment was not clearly confirmed. We suggest that the Cu-‘‘stretching’’ modes are to be expected at higher frequencies (between 210 cm^{-1} and 270 cm^{-1}) in all layered copper oxides.

The lines observed at 231 (229) cm^{-1} and 320 (327) cm^{-1} in SrCuO_2 ($\text{Sr}_{0.5}\text{Ca}_{0.5}\text{CuO}_2$) we assign to $\text{O}_{\text{Sr}} B_{1g}$ and $\text{O}_{\text{Sr}} B_{3g}$ modes, respectively. The relatively large difference in the frequencies of these two modes is due to the fact that the former vibration is perpendicular to the chains, whereas the latter is along the chains. The O_{Sr} atom could be viewed as an ‘‘apex’’ for the chains with an environment similar to that of apex oxygen O4 in $R\text{Ba}_2\text{Cu}_3\text{O}_7$ and $R\text{Ba}_2\text{Cu}_4\text{O}_8$ (R represents rare earth). In $\text{YBa}_2\text{Cu}_3\text{O}_7$ the nondiagonal B_{2g} and B_{3g} modes of the apex oxygen exhibit the strongest intensities among the nondiagonal modes and were reported at 210 cm^{-1} and 303 cm^{-1} .^{20,23} Their frequencies are close to those of the ‘‘apex’’ O_{Sr} mentioned above for $\text{Sr}_{1-x}\text{Ca}_x\text{CuO}_2$. On the other hand, in $\text{YBa}_2\text{Cu}_4\text{O}_8$ the two strongest non-diagonal modes were observed at 228 cm^{-1} and 314 cm^{-1} , but there they were assigned to the chain O1 B_{3g} and chain Cu1 B_{2g} modes.¹⁵ An argument for that assignment was the decreasing of the relative intensity of chain-related lines in $\text{Y}_2\text{Ba}_4\text{Cu}_7\text{O}_{15-\delta}$ compared to $\text{YBa}_2\text{Cu}_4\text{O}_8$ (i.e., a doubled concentration of chains in the latter compound). Käll *et al.*¹⁸ noted that this could be caused by an enhanced polarizability of the ‘‘apex’’ O4 bonds due to double chains in these compounds. In light of the similarities of these frequencies in these compounds this latter interpretation suggests that these two lines in all above-mentioned structures originate from the ‘‘apex’’ oxygen nondiagonal modes.

The line at 120 cm^{-1} in SrCuO_2 we assign to the B_{3g} Sr mode. Similarly to the other observed Sr mode (A_g at 188 cm^{-1}) this line must broaden and shift to higher frequencies in the case of $\text{Sr}_{0.5}\text{Ca}_{0.5}\text{CuO}_2$. The calculated frequency for this mode in the Ca-substituted compound is 138 cm^{-1} , but it is difficult to assign the weak and broad structure near 150 cm^{-1} in the yz spectrum to this mode.

The hypothesis for unmixed Raman-active modes (i.e., each mode contains vibrations of only one type of atom) is confirmed by our lattice-dynamics calculations for almost all Raman-active modes. We expected to find the Sr B_{1g} mode close to or even higher in frequency than the Sr B_{3g} mode taking into account the anisotropic oxygen environment of Sr. To our surprise we observed in both samples a very narrow line (line width $\Gamma = 6\text{ cm}^{-1}$ in SrCuO_2 and $\Gamma = 8\text{ cm}^{-1}$ in $\text{Sr}_{0.5}\text{Ca}_{0.5}\text{CuO}_2$) at a very low frequencies (78 and 84 cm^{-1}) and with small shift (6 cm^{-1}) between the two samples. The lattice-dynamics calculations predict indeed the presence of such low-frequency B_{1g} mode (75 and 80 cm^{-1} , see Table II). In this mode all nearest Sr, O_{Sr} , Cu, and O_{Cu} atoms vibrate in-phase along the x axis. It is possible to explain the low frequency of this mode using the following arguments. In some cases it is helpful for the analysis of structures which contain relatively isolated units, to use a molecular-site group-theoretical analysis.^{24,25} In our case we can consider the crystal structure as one containing infinite $(\text{Cu}_2\text{O}_4)_n$ molecules with Sr atoms between them. Making the correlation between the modes of the free infinite $(\text{Cu}_2\text{O}_4)_n$ molecule and the modes in the crystal, it appears that one molecular rotational mode (around the molecular axis) with, naturally, rather low frequency must be transformed into one B_{1g} crystal librational mode. Note also that some similarity may be found between this mode and the TA mode in the Y point in the cubic SrO (out-of-phase translations of the adjacent Sr-O layers), where the frequency of this TA mode is 120 cm^{-1} .¹⁶

The remaining two nondiagonal modes (those of O_{Cu}) have so far not been observed. For the B_{3g} O_{Cu} stretching mode the calculated frequency for both compounds is 539 cm^{-1} and 562 cm^{-1} , respectively. For the last B_{1g} mode the lattice-dynamics calculations show that this mode is a mixture of out-of-phase vibrations of O_{Cu} and O_{Sr} along the x direction with frequency below 200 cm^{-1} .

D. IR-active phonons

The room temperature infrared reflectivity spectra of SrCuO_2 and $\text{Sr}_{0.5}\text{Ca}_{0.5}\text{CuO}_2$ are shown in Fig. 4(a). The information on the frequency dependence of the dynamical dielectric function was obtained by a Kramers-Kronig analysis of the reflectivity. The data for the imaginary part of the dielectric function and the loss function, the maxima of which yield positions of the transverse and the longitudinal optical phonons, respectively, are shown in Fig. 4(b) and 4(c). The experimental and the calculated TO and LO frequencies of the IR-active phonons as well as their assignment are summarized in Table III.

We comment first on the B_{1u} O_{Cu} vibration. This mode consists of out-of-phase antistretching vibrations of O_{Cu} and Cu along the chains (z direction), and it has analogs in all chain-containing copper oxides. Its TO frequency depends

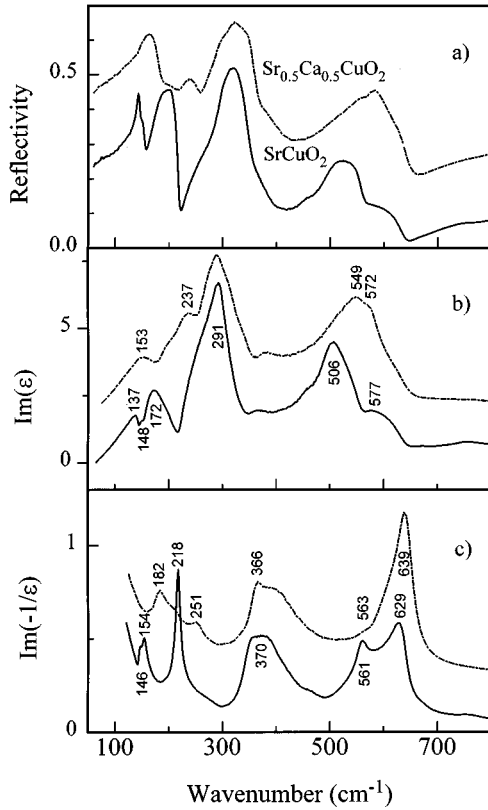


FIG. 4. (a) Room temperature far-infrared reflectivity spectra of SrCuO_2 (solid line) and $\text{Sr}_{0.5}\text{Ca}_{0.5}\text{CuO}_2$ (dotted line). (b) and (c) Spectral dependence of the imaginary part of the dielectric function and the loss function. The curves for $\text{Sr}_{0.5}\text{Ca}_{0.5}\text{CuO}_2$ are shifted for clarity by 0.2 (a), 2 (b), and 0.3 (c).

primarily on the Cu-O distance along the chains and only weakly on the other environment of these atoms. Indeed, in Ca_2CuO_3 the frequency of this mode is 682 cm^{-1} (the distance $d_{\text{Cu-O}} = 1.89\text{ \AA}$),¹³ in $\text{Ca}_{1.8}\text{Sr}_{0.2}\text{CuO}_3$ it decreases to 660 cm^{-1} .¹² In the case of highly doped superconducting materials of the $\text{RBa}_2\text{Cu}_3\text{O}_7$ family [except $R = \text{Pr}$ (Ref. 26)] it is hardly possible to experimentally observe similar oxygen stretching vibrations from the chains or planes (normal to the c axis with B_{2u} or B_{3u} symmetry) due to the

screening effects. However, for some of them data are available from neutron scattering experiments.²⁷ The frequencies of the corresponding modes are in the range $552\text{--}566\text{ cm}^{-1}$ ($d_{\text{Cu-O}} \approx 1.94\text{ \AA}$ for all of them). Therefore, in our samples $\text{Sr}_{0.5}\text{Ca}_{0.5}\text{CuO}_2$ ($d_{\text{Cu-O}} = 1.94\text{ \AA}$) and SrCuO_2 ($d_{\text{Cu-O}} = 1.96\text{ \AA}$) we assign the TO lines observed at 549 cm^{-1} and 506 cm^{-1} to this mode, respectively.

Based on the lattice-dynamics calculations we assign the observed highest-frequency line at 577 cm^{-1} in SrCuO_2 and at 572 cm^{-1} (not clearly resolved) in $\text{Sr}_{0.5}\text{Ca}_{0.5}\text{CuO}_2$ to the B_{2u} mode of O_{Cu} . The corresponding mode involving chain-oxygen vibrations normal to the chains in double-chained $\text{YBa}_2\text{Cu}_4\text{O}_8$ (of B_{1u} symmetry in this case) is expected at higher frequency because of the shortening of the Cu-O distances. Such a phonon was indeed observed in $\text{YBa}_2\text{Cu}_4\text{O}_8$ (at 598 cm^{-1}) where, based on a comparison between $\text{YBa}_2\text{Cu}_3\text{O}_7$ and $\text{YBa}_2\text{Cu}_4\text{O}_8$, it was assigned to the apex oxygen vibration.^{28,29} In view of the arguments presented here it is likely that this peak instead belongs to the O_{Cu} vibration whereas the apex oxygen vibration is at 512 cm^{-1} . This point was also made by Buckley *et al.*³⁰ based on the lattice-dynamics calculations of Yim *et al.*³¹

The broad reststrahlen-band observed in the range $291\text{--}370\text{ cm}^{-1}$ in SrCuO_2 and $288\text{--}366\text{ cm}^{-1}$ in $\text{Sr}_{0.5}\text{Ca}_{0.5}\text{CuO}_2$ [derived from the TO and LO values in Figs. 4(b) and 4(c)] we assign to the B_{1u} mode of O_{Sr} (bending vibration along z). The line with the largest shift between the Ca-free [TO (LO) frequency is 172 (218) cm^{-1}] and Ca-substituted sample [TO (LO) 237 (251) cm^{-1}] we assign to the B_{3u} mode involving primarily out-of-phase vibrations of O_{Sr} and Sr atoms along the x direction.

The calculations also predict the existence of two low-frequency modes (at 124 and 150 cm^{-1} for SrCuO_2) with a rather small TO-LO splitting. In the experimental spectrum of SrCuO_2 we can find indeed two peaks at 137 and 148 cm^{-1} (TO frequencies). In the case of $\text{Sr}_{0.5}\text{Ca}_{0.5}\text{CuO}_2$ one resolves only one peak at 153 cm^{-1} .

IV. SUMMARY

Far-infrared reflectivity and polarized micro-Raman spectra of $\text{Sr}_{1-x}\text{Ca}_x\text{CuO}_2$ ($x = 0, 0.5$) ceramic samples were presented. The assignment of the observed lines to definite atomic vibrations was made based on shell model lattice-

TABLE III. Experimental and calculated frequencies (in cm^{-1}) and an assignment of the infrared-active modes.

Type	SrCuO_2				$\text{Sr}_{1-x}\text{Ca}_x\text{CuO}_2$				Assignment
	Expt.		Calc.		Expt.		Calc.		
	TO	LO	TO	LO	TO	LO	TO	LO	
B_{1u}	148	154	150	158	153	182	167	174	$+6\text{Cu}^z - 5\text{Sr}^z + 5\text{O}_{\text{Cu}}^z$
B_{1u}	291	370	304	384	288	366	314	403	$+16\text{O}_{\text{Sr}}^z - 3\text{Cu}^z + 3\text{O}_{\text{Cu}}^z$
B_{1u}	506	561	456	563	549	563	504	588	$+16\text{O}_{\text{Cu}}^z - 5\text{O}_{\text{Sr}}^z - 3\text{Cu}^z$
B_{2u}	-	-	202	207	-	-	232	235	$+6\text{Cu}^y - 5\text{Sr}^y + 5\text{O}_{\text{Cu}}^y$
B_{2u}	-	-	429	535	-	-	432	542	$+15\text{O}_{\text{Sr}}^y + 6\text{O}_{\text{Cu}}^y - 4\text{Cu}^y$
B_{2u}	577	629	549	572	572	639	543	566	$+15\text{O}_{\text{Cu}}^y - 8\text{O}_{\text{Sr}}^y - 2\text{Cu}^y$
B_{3u}	137	146	124	130	-	-	120	137	$+7\text{O}_{\text{Sr}}^x - 7\text{O}_{\text{Cu}}^x - 6\text{Cu}^x + 4\text{Sr}^x$
B_{3u}	172	218	172	210	237	251	181	209	$+12\text{O}_{\text{Sr}}^x - 4\text{Sr}^x + 4\text{Cu}^x - 3\text{O}_{\text{Cu}}^x$
B_{3u}	-	-	297	443	-	-	303	455	$+12\text{O}_{\text{Cu}}^x + 11\text{O}_{\text{Sr}}^x - 2\text{Cu}^x - 2\text{Sr}^x$

dynamics calculations and discussed by comparing these compounds with similar copper oxides.

ACKNOWLEDGMENTS

We thank L. N. Bozukov for the x-ray diffraction measurements. M.V.A. and A.P.L. acknowledge financial sup-

port from the Alexander von Humboldt Foundation (Bonn, Germany) and from the European Community (ERBCHICT-941659), respectively. They thank the Institut für Festkörperphysik (TU-Berlin) for its hospitality. This work was supported in part by Grant No. F530 (NIS 2241) of the Bulgarian National Science Fund.

- *Permanent address: Faculty of Physics, Sofia University, BG-1126 Sofia, Bulgaria.
- ¹Z. Hiroi, M. Takano, M. Azuma, Y. Takeda, and Y. Bando, *Physica C* **185-189**, 523 (1991).
 - ²M. Marezio and J. Chenavas, *J. Solid State Chem.* **121**, 24 (1996).
 - ³R. S. Roth, C. J. Rawn, J. Ritter, and B. P. Burton, *J. Am. Ceram. Soc.* **72**, 1545 (1989).
 - ⁴P. Karen, O. Braaten, and A. Kjekshus, *Acta Chem. Scand.* **46**, 805 (1992).
 - ⁵M. Matsuda and K. Katsumata, *J. Magn. Magn. Mater.* **140-145**, 1671 (1995).
 - ⁶N. Motoyama, H. Eisaki, and S. Uchida, *Phys. Rev. Lett.* **76**, 3212 (1996).
 - ⁷M. Kato, K. Shiota, and Y. Koike, *Physica C* **258**, 284 (1996).
 - ⁸T. M. Rice, S. Gopalan, and M. Sigrist, *Europhys. Lett.* **23**, 445 (1993).
 - ⁹Chr. L. Teske and Hk. Müller-Buschbaum, *Z. Anorg. Allg. Chem.* **379**, 234 (1970).
 - ¹⁰Y. Matsushita, Y. Oyama, M. Hasegawa, and H. Takei, *J. Solid State Chem.* **114**, 289 (1994).
 - ¹¹J. Liang, Z. Chen, F. Wu, and S. Xie, *Solid State Commun.* **75**, 247 (1990).
 - ¹²M. Yoshida, S. Tajima, N. Koshizuka, S. Tanaka, S. Uchida, and S. Ishibashi, *Phys. Rev. B* **44**, 11 997 (1991).
 - ¹³G. A. Zlateva, V. N. Popov, M. Gyulmezov, L. N. Bozukov, and M. N. Iliev, *J. Phys.: Condens. Matter* **4**, 8543 (1992).
 - ¹⁴O. V. Misochko, S. Tajima, C. Urano, H. Eisaki, and S. Uchida, *Phys. Rev. B* **53**, 14 733 (1996).
 - ¹⁵E. T. Heyen, R. Liu, C. Thomsen, R. Kremer, M. Cardona, J. Karpinski, E. Kaldis, and S. Rusiecki, *Phys. Rev. B* **41**, 11 058 (1990).
 - ¹⁶V. N. Popov, *J. Phys. Condens. Matter* **7**, 1625 (1995).
 - ¹⁷C. R. A. Catlow, W. C. Mackrodt, M. J. Norgett, and A. M. Stoneham, *Philos. Mag.* **35**, 177 (1977).
 - ¹⁸M. Käll, A. P. Litvinchuk, P. Berastegui, L. -G. Johansson, L. Börjesson, M. Kakihana, and M. Osada, *Phys. Rev. B* **53**, 3590 (1996).
 - ¹⁹V. G. Hadjiev, M. V. Abrashev, M. N. Iliev, and L. N. Bozukov, *Physica C* **171**, 257 (1990).
 - ²⁰K. F. McCarty, J. Z. Liu, R. N. Shelton, and H. B. Radousky, *Phys. Rev. B* **41**, 8792 (1990).
 - ²¹W. Kress, U. Schröder, J. Prade, A. D. Kulkarni, and F. W. de Wette, *Phys. Rev. B* **38**, 2906 (1988).
 - ²²O. V. Misochko, S. Tajima, S. Miyamoto, H. Kobayashi, S. Kagiya, N. Watanabe, N. Koshizuka, and S. Tanaka, *Phys. Rev. B* **51**, 1346 (1995).
 - ²³B. Friedl, C. Thomsen, E. Schönherr, and M. Cardona, *Solid State Commun.* **76**, 1107 (1990).
 - ²⁴M. V. Abrashev, G. A. Zlateva, M. N. Iliev, and M. Gyulmezov, *Phys. Rev. B* **49**, 11 783 (1994).
 - ²⁵Yu. E. Kitaev, M. F. Limonov, A. G. Panfilov, R. A. Evarestov, and A. P. Mirgorodsky, *Phys. Rev. B* **49**, 9933 (1994).
 - ²⁶J. Humlicek, A. P. Litvinchuk, W. Kress, B. Lederle, C. Thomsen, M. Cardona, H.-U. Habermeier, I. E. Trofimov, and W. König, *Physica C* **206**, 345 (1993).
 - ²⁷L. Pintschovius and W. Reichardt, in *Physical Properties of High Temperature Superconductors IV*, edited by D. M. Ginsberg (World Scientific, Singapore, 1994), p. 295.
 - ²⁸A. P. Litvinchuk, C. Thomsen, P. Murugaraj, and M. Cardona, *Z. Phys. B* **86**, 329 (1992).
 - ²⁹C. Thomsen, A. P. Litvinchuk, E. Schönherr, and M. Cardona, *Phys. Rev. B* **45**, 8154 (1992).
 - ³⁰R. J. Buckley, M. P. Staines, and H. J. Trodahl, *Physica C* **193**, 33 (1992).
 - ³¹K. K. Yim, J. Oitmaa, and M. M. Elcombe, *Solid State Commun.* **77**, 385 (1991).